Rapid and Reversible Block of N-Type Calcium Channels (Ca_V 2.2) by ω-Conotoxin GVIA in the Absence of Divalent Cations

Haoya Liang and Keith S. Elmslie

Department of Physiology, Tulane University Health Science Center, New Orleans, Louisiana 70112

ω-Conotoxin GVIA (ωCGVIA) has been reported to be an irreversible blocker of N-type calcium channels (Ca_V 2.2). However, recent studies have demonstrated that the ωCGVIA off-rate is correlated with divalent cation concentration, because increasing $[Ba^{2+}]_o$ accelerated the recovery from ωCGVIA block. This predicts that the dissociation of ωCGVIA from N-channels will be negligible in the absence of divalent cations. Surprisingly, we find that ωCGVIA block is rapidly reversible in divalent cation-free (0 Ba^{2+}) external solutions in which current was carried by MA^+. The recovery followed a single-exponential time course with $\tau = 31$ sec. Isochronic measurements showed that, at 2 min after the removal of toxin, current returned to 86% of control in 0 Ba^{2+} compared with 19% in 3 mM Ba^{2+}. The off-rate of ωCGVIA from N-channels was dependent on $[Ba^{2+}]_o$, because, at an intermediate concentration (3 μM Ba^{2+}), N-current recovered with $\tau = 64$ sec, significantly slower than that in 0 Ba^{2+} but faster than in 3 mM Ba^{2+}. Recovery from ωCGVIA block was also observed when Cs^+ or Na^+ carried the current in divalent cation-free conditions. The off-rate was sensitive to $[Ba^{2+}]_o$ only during washout, because current recovered slowly in the presence of 3 mM Ba^{2+}, even after it was blocked in 0 Ba^{2+}. Assuming that the toxin is a pore blocker, our findings are consistent with a model in which Ba^{2+} interacts at a site on the extracellular surface of the channel to regulate ωCGVIA dissociation from N-channels.

Key words: bullfrog; sympathetic neurons; patch-clamp; monovalent cations; toxin; off-rate; on-rate

Voltage-gated calcium channels with distinct biophysical properties have evolved to accommodate the complexity of neuronal functions. To evaluate the contributions from each type of calcium channel and to study these channels in detail, specific blockers have been used. Peptide toxins have greatly facilitated the identification of voltage-gated calcium channels by targeting the pore-forming α_1 subunits.

ω-Conotoxin GVIA (ωCGVIA) is a potent N-type calcium channel blocker. It was first shown in radiolabeled binding assays to bind brain synaptosomes with a half-saturation concentration in the subnanomolar range (Cruz and Olivera, 1986). Dissociation of toxin from its binding site was undetectable with prolonged washout (up to several hours). The presence of millimolar concentrations of divalent cations inhibited the formation of the toxin–receptor complex but did not affect the toxin off-rate (Cruz and Olivera, 1986; Wagner et al., 1988; Witcher et al., 1993). The effect of divalent cations on toxin binding to channels was corroborated in functional experiments in rat and frog sympathetic neurons in which increasing external divalent cation concentration slowed the rate of N-current block (Boland et al., 1994; Elmslie et al., 1994). In addition, these experiments showed that high divalent cation concentrations accelerated the recovery from ωCGVIA block. The effects of divalent cations have been suggested to arise from screening of surface charge and/or interaction between divalent cations and N-channels at extracellular sites (Boland et al., 1994).

ωCGVIA is a basic 27 amino acid peptide that carries a net +5 charge. Several amino acid residues have been implicated in binding of ωCGVIA to N-channels, among which Lys2 and Tyr13 have been shown to be important for high-affinity interaction between the toxin and the channel (Kim et al., 1995; Lew et al., 1997). The tertiary structure of the toxin is highly stabilized by three intramolecular disulfide bridges. A putative ωCGVIA receptor site on N-channels has also been identified in the external loop between the membrane-spanning segment S5 and pore-lining segment H5 in domain III. Mutations within this region altered the kinetics of ωCGVIA block (Ellinor et al., 1994; Feng et al., 2001b). The location of the toxin-binding domain is consistent with the idea that the toxin works as a pore blocker (Boland et al., 1994; Ellinor et al., 1994).

The mechanism by which divalent cations modify ωCGVIA binding to N-channels has aroused much speculation. Given the effects of divalent cations on toxin kinetics, one prediction is that the binding of ωCGVIA should be faster in divalent cation-free solutions than in the presence of divalent cations, and the block should be virtually irreversible after removal of toxin. These predictions were tested in divalent cation-free solutions using methylammonium (MA^+) as the charge carrier. Results from our experiments provide evidence supporting the idea that divalent cations act at a site(s) on the extracellular surface of the channel to alter ωCGVIA kinetics. Thus, it appears that divalent cation binding to the channel induces conformational changes that are reflected by toxin off-rate.

MATERIALS AND METHODS

Cells. Paravertebral sympathetic ganglia were isolated from adult bullfrogs (*Rana catesbeiana*). The method by which they were killed was approved by the Institutional Animal Care and Usage Committee. Neu-

Received May 28, 2002; revised July 25, 2002; accepted Aug. 1, 2002.

This work was supported by National Institutes of Health Grant NS33671 (K.S.E.).

Correspondence should be addressed to Keith S. Elmslie, Department of Physiology, Tulane University Health Science Center, 1430 Tulane Avenue, New Orleans, LA 70112. E-mail: kelmslie@tulane.edu.

H. Liang's present address: Johns Hopkins University School of Medicine, Department of Biomedical Engineering and Neuroscience, Ross 713, 720 Rutland Avenue, Baltimore, MD 21205.

Table 1. Composition of external solutions (in mM)

External solutions	0 Ba^{2+}–MA^+	0 Ba^{2+}–Cs^+	0 Ba^{2+}–Na^+	3 μM Ba^{2+}–MA^+	3 mM Ba^{2+}–MA^+	3 mM Ba^{2+}–NMG^+
MA·Cl	90	–	–	90	90	–
Cs·Cl	–	90	–	–	–	–
Na·Cl	–	–	90	–	–	–
NMG·HEPES	10	10	10	10	10	10
NMG·HEDTA	10	10	10	10	–	–
NMG·Cl	–	–	–	–	30	115
$Ba·Cl_2$	–	–	–	0.09	3	3

The concentration of Ba^{2+} added to make the buffered 3 μM Ba^{2+} external solution was calculated from the stability constant of HEDTA (Martell and Smith, 1974) using a computer program based on Fabiato and Fabiato (1979). This program, written by H. Liang, determined the concentration of the divalent cation to be added to a solution given the desired final concentration and the chelator to be used.

rons were dissociated with collagenase–dispase digestion and trituration (Kuffler and Sejnowski, 1983; Jones, 1987; Elmslie, 1992). Cells were maintained at 4°C for 1–14 d in L-15 medium supplemented with 10% fetal bovine serum and penicillin–streptomycin.

Electrophysiology. Neurons were voltage clamped in the whole-cell configuration of the patch-clamp technique. Pipettes were pulled from either Corning 7052 (Corning, NY) or Schott 8250 glass on a Sutter Instruments (Novato, CA) P-97 puller. Series resistance ranging from 0.3 to 1.5 MΩ was compensated at 95%. Currents were recorded using an Axopatch 200A amplifier (Axon Instruments, Foster City, CA). Experiments were controlled with either a Macintosh IIci or a Macintosh 800 computer (Apple Computer, Cupertino, CA) running S3 data acquisition software written by Dr. Stephen Ikeda (National Institutes of Health, National Institute on Alcohol Abuse and Alcoholism, Bethesda, MD). Currents were digitized with a MacAdios II analog-to-digital converter (GW Instruments, Somerville, MA) and stored on a hard disk. Leak current was on-line subtracted using a P/4 or P/8 protocol. Step currents were sampled at 50 kHz and were typically filtered at 10 kHz. All recordings were performed at 25°C.

Solutions. To isolate calcium currents, Na^+ and K^+ were replaced in the internal and external solutions with an impermeant cation, *N*-methyl-D-glucamine (NMG^+). The internal solution contained the following (in mM): 65.5 NMG·Cl, 6.0 $Mg·Cl_2$, 14 creatine·PO_4, 2.5 NMG·HEPES, 5 $Tris_2$·ATP, and 10 NMG·EGTA. When examining monovalent cation permeation through N-channels, we typically replaced NMG^+ in the external solution with MA^+ (Jones and Marks, 1989a,b). In several studies, however, Cs^+ and Na^+ were used as external monovalent cations. The isolation of N-current was best in MA^+ and worst in Na^+, with Cs^+ being intermediate (see Results). Because we were interested only in toxin binding and unbinding kinetics, contaminating currents should not be a problem. When Na^+ was used as the charge carrier, the external solution also contained 2 μM tetrodotoxin (TTX) to block voltage-dependent sodium channels. The compositions of the different external solutions are listed in Table 1. As a result of the large number of external solutions used in these experiments, each solution is referred to by its Ba^{2+} concentration and dominant monovalent cation (Table 1). The osmolarity of the internal solution was 230 mOsm, and that of the external solutions ranged from 220 to 240 mOsm. All solutions were titrated to pH 7.2 with NMG^+ base.

Chemicals. ωCGVIA was obtained from Bachem Bioscience (King of Prussia, PA), and TTX was from Calbiochem (San Diego, CA). All other chemicals were obtained from Sigma (St. Louis, MO).

Data analysis. Data were analyzed using Igor Pro (WaveMetrics, Lake Oswego, OR) running on a Macintosh computer. The step current was measured as the average of 10 points at the end of the 10 msec voltage step. Fractional block was equal to $1 - (I_{\text{during block}}/I_{\text{control}})$. Group data were calculated as mean ± SD throughout the study. ANOVA was used for statistical analysis of data from multiple groups, with the Tukey's honestly significant difference test used to determine significance among the groups being compared. Student's *t* test was used when testing the significance between two groups. The ANOVA was performed using IGOR Pro, and the *t* test was done using Excel (Microsoft, Seattle, WA).

RESULTS

Isolation of calcium current with MA^+

To study the effects of divalent cations on the kinetics of ωCGVIA, block of N-channels was compared in the presence and absence of Ba^{2+}. MA^+ was the charge carrier in the divalent cation-free solution (0 Ba^{2+}). This monovalent cation was chosen because it provides better calcium current isolation than the smaller inorganic cations, which can permeate both calcium channels and noncalcium channels, such as sodium and potassium channels (see below) (Jones and Marks, 1989a,b).

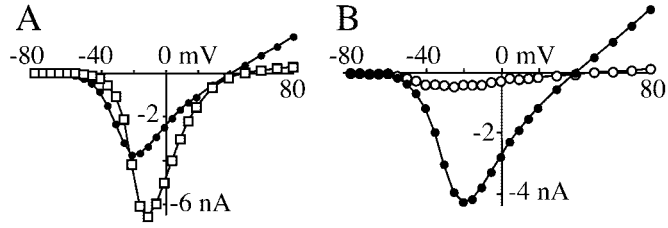

Figure 1. Calcium current properties in the absence of divalent cations. *A*, *I–V* for 0 Ba^{2+}–MA^+ (●) and 3 mM Ba^{2+}–NMG^+ (□) are shown from the same cell. Peak current in 0 Ba^{2+} occurs ~10 mV hyperpolarized to that in 3 mM Ba^{2+}. Note that the current is smaller in 0 Ba^{2+} than in 3 mM Ba^{2+}. *B*, The *I–V* in 0 Ba^{2+}–MA^+ is shown before (●) and after (○) application of 3 μM ωCGVIA. ωCGVIA blocks outward current to the same extent as it does inward current.

Comparison of the current–voltage relationship (*I–V*) in 3 mM and 0 Ba^{2+} showed that the *I–V* in 0 Ba^{2+}–MA^+ was shifted ~10 mV hyperpolarized to that in 3 mM Ba^{2+}–NMG^+. In addition, peak current amplitude decreased when switching from 3 mM Ba^{2+} to 0 Ba^{2+} (Fig. 1*A*). Application of 3 μM ωCGVIA reduced peak current in 0 Ba^{2+}–MA^+ by 88 ± 3% ($n = 10$) (Figs. 1*B*, 2*B*), which was statistically similar to that in 3 mM Ba^{2+}–NMG^+ (86 ± 3%; $n = 7$) (Fig. 2*A*). The percentage of ωCGVIA-sensitive N-current is consistent with previous findings (Elmslie et al., 1992; Liang and Elmslie, 2001). In 0 Ba^{2+}–MA^+, a large outward current was recorded at strong depolarized potentials. ωCGVIA reduced this outward current to the same extent as the inward current, suggesting that it was also carried through N-channels. The ion carrying this current is presumed to be MA^+ because there is no other permeant cation. Jones and Marks (1989a) also observed an outward current in their recordings using MA^+ and speculated that it resulted from MA^+ that entered the cell through the relatively leaky membrane that is typical of recordings in the absence of divalent cations. Jones and Marks (1989a,b) also observed the outward N-current when other monovalent cations were used as charge carriers. We confirmed these observations in our recordings using Cs^+ or Na^+ as charge carriers (data not shown). The ability of ωCGVIA to block the same fraction of whole-cell current in both 0 Ba^{2+}–MA^+ and 3 mM Ba^{2+}–NMG^+ demonstrates that N-type calcium current is well isolated with MA^+ as the charge carrier.

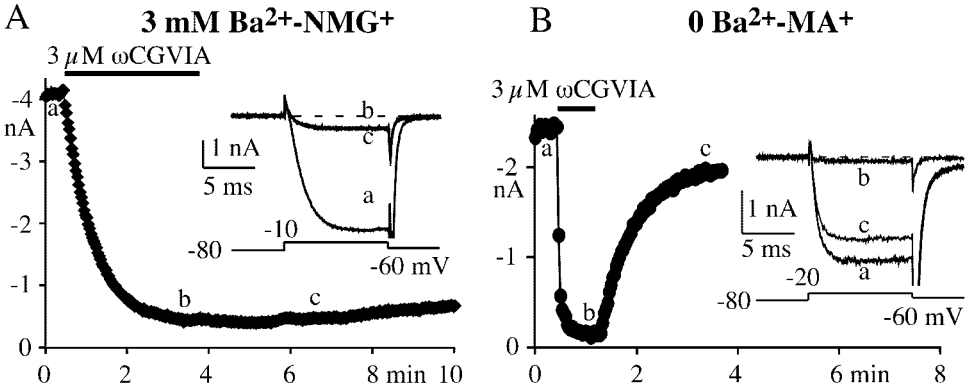

Figure 2. A comparison of the kinetics of ωCGVIA block in 3 mM Ba^{2+}–NMG^+ and 0 Ba^{2+}–MA^+. *A*, The time course of N-current block by ωCGVIA in 3 mM Ba^{2+}–NMG^+. ωCGVIA application is indicated by the *solid bar*. The *inset* shows current during voltage steps to −10 mV before (*a*), during (*b*), and 3 min after (*c*) removal of ωCGVIA. *B*, The time course of ωCGVIA block of N-current in 0 Ba^{2+}–MA^+. Note that both the time course of block and the recovery from block are faster in 0 Ba^{2+} than in 3 mM Ba^{2+}. The *inset* shows currents as described for *A*.

Kinetics of ωCGVIA block in 3 mM Ba^{2+} and 0 Ba^{2+}

Although at steady state 3 μM ωCGVIA blocked whole-cell calcium current to the same extent in 0 Ba^{2+} and 3 mM Ba^{2+}, the block developed with distinctive time courses. In 3 mM Ba^{2+}–NMG^+ (Fig. 2*A*), the onset of block could be fit according to a single-exponential function, with a mean time constant (τ) of 35 ± 11 sec ($n = 7$). In 0 Ba^{2+}–MA^+, the block was more rapid than in 3 mM Ba^{2+} and reached steady state almost within the interval of 2 sec between voltage steps (Fig. 2*B*). The toxin blocking τ was estimated from single-exponential fits to be 1.9 ± 1 sec ($n = 10$). However, this number is likely to be an overestimate, because the on-rate was limited by both the step interval (2 sec) and the exchange time of our flow device (~2 sec).

An acceleration of ωCGVIA blocking rate in the absence of divalent cations is consistent with previous studies. However, surprisingly, the recovery from ωCGVIA block was also accelerated in 0 Ba^{2+} (Fig. 2*B*). The time course of N-current recovery in 0 Ba^{2+}–MA^+ could be fit with a single-exponential function with an average $\tau = 31 \pm 10$ sec ($n = 10$). Not only was the dissociation of ωCGVIA from the channels faster in 0 Ba^{2+}, but it was also nearly complete (86 ± 7% of control; $n = 10$) by the end of the wash-off period (2 min). However, very little current recovered in 3 mM Ba^{2+}–NMG^+, even after extended wash off (Fig. 2*A*). Because of the slow and incomplete toxin washout in 3 mM Ba^{2+}–NMG^+, we were unable to obtain reliable estimates of the recovery τ using single-exponential fitting. In addition, prolonged wash off was complicated with rundown, which tends to mask the current recovery from ωCGVIA block. Therefore, isochronic measurement was used to compare recovery during the first few minutes of washout in 3 mM Ba^{2+}–NMG^+ with that in 0 Ba^{2+}–MA^+. Two minutes after the start of wash off, current returned to 19 ± 8% ($n = 6$) of control in 3 mM Ba^{2+}, which is significantly different from the 86 ± 7% ($n = 10$) of control in 0 Ba^{2+} ($p < 0.05$).

Ba^{2+} slows ωCGVIA kinetics

To reach the conclusion that the presence of Ba^{2+} altered ωCGVIA-blocking kinetics, we had to rule out an alternative possibility. The main monovalent cation in our typical 3 mM Ba^{2+} solution differed from that in 0 Ba^{2+} (NMG^+ vs MA^+, respectively) (Table 1). Thus, the differences in the kinetics of ωCGVIA block in 3 mM Ba^{2+}–NMG^+ versus 0 Ba^{2+}–MA^+ solutions could arise from the different monovalent cations rather than Ba^{2+}. To determine which cation alters ωCGVIA kinetics, NMG^+ in the 3 mM Ba^{2+} external solution was replaced with MA^+. The *I–V* in the 3 mM Ba^{2+}–MA^+ solution (data not shown) had the same properties as that in 3 mM Ba^{2+}–NMG^+. In

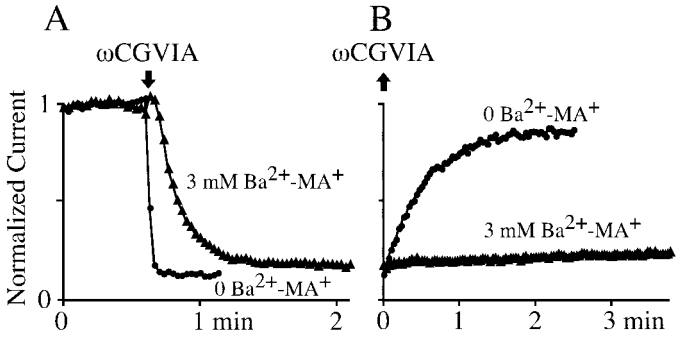

Figure 3. Ba^{2+} is the crucial factor in determining the kinetics of toxin block. Unlike in the previous figures, the 3 mM Ba^{2+} external solution used in these experiments contained MA^+ as the monovalent cation, which made Ba^{2+} concentration the only variable between the two test solutions. *A*, Time course of ωCGVIA block in 0 Ba^{2+}–MA^+ (●) and 3 mM Ba^{2+}–MA^+ (▲) in the same cell. Currents were normalized to control. The *solid downward arrow* marks the application of 3 μM ωCGVIA. *B*, Time course of recovery from ωCGVIA block in 0 Ba^{2+}–MA^+ (●) and 3 mM Ba^{2+}–MA^+ (▲) in the same cell as in *A*. Currents were normalized to control. The *upward arrow* marks the removal of 3 μM ωCGVIA. Time 0 is the first point after wash off starts.

the 3 mM Ba^{2+}–MA^+ external solution, 88 ± 4% ($n = 4$) of current was blocked by ωCGVIA (Fig. 3*A*), which was similar to toxin block in both 3 mM Ba^{2+}–NMG^+ and 0 Ba^{2+}–MA^+. The mean blocking τ in 3 mM Ba^{2+}-MA^+ was 10 ± 1 sec ($n = 4$), which was significantly ($p < 0.01$) smaller than that in 3 mM Ba^{2+}–NMG^+. However, the recovery from ωCGVIA block was slow and incomplete (Fig. 3*B*). At 2 min after wash off began, the current returned to 19 ± 3% ($n = 4$) of control, which was similar to that observed in the 3 mM Ba^{2+}–NMG^+ external solution. The results support the idea that the presence of Ba^{2+} slows the kinetics of ωCGVIA block.

ωCGVIA block is reversible with inorganic monovalent cations

Our assumption has been that MA^+ is inert with respect to the channel and toxin. However, this may not be the case, because the blocking time course is significantly faster in 3 mM Ba^{2+}–MA^+ than in the 3 mM Ba^{2+}–NMG^+ external solution (10 vs 35 sec, respectively). Thus, we examined the effect of inorganic monovalent cations, Cs^+ and Na^+, on ωCGVIA block of N-channels (Fig. 4). Using Cs^+ as the charge carrier (0 Ba^{2+}–Cs^+), the percentage block of peak current by 3 μM ωCGVIA (83 ± 1%; $n = 4$) was slightly less than when either MA^+ or Ba^{2+} was the charge carrier. However, the percentage block in 0 Ba^{2+}–Na^+ (56 ± 10%; $n = 12$) was significantly lower than with any other

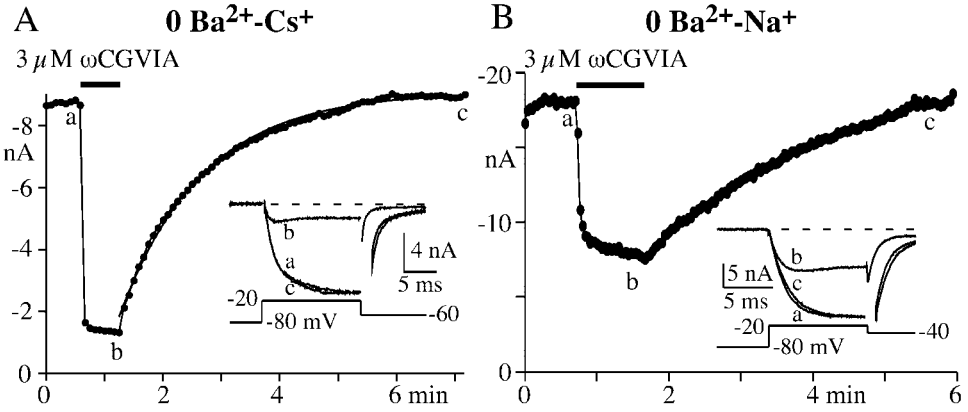

Figure 4. ωCGVIA block is reversible when Cs^+ or Na^+ permeates N-channels. The time course of block and recovery from block are shown in both 0 Ba^{2+}–Cs^+ (*A*) and 0 Ba^{2+}–Na^+ (*B*). The *solid bars* indicate the application of ωCGVIA. For each *panel*, the recovery time course is fit to a single-exponential equation with $\tau = 85$ sec (*A*) and 179 sec (*B*). The *lowercase letters* indicate the time from which the records shown in the *inset* were taken. The *inset* currents are shown before (*a*), during (*b*), and after recovery from (*c*) the application of 3 μM ωCGVIA.

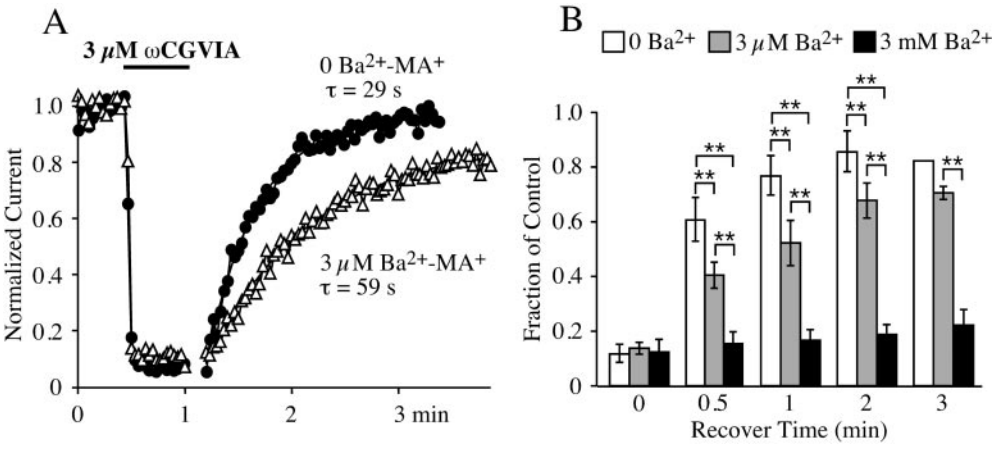

Figure 5. Ba^{2+} at 3 μM slows the recovery of N-current from ωCGVIA block. *A*, The time course of ωCGVIA block and the recovery from toxin block in 0 Ba^{2+}–MA^+ (●) and 3 μM Ba^{2+}–MA^+ (△) in the same cell. Currents were normalized to the current amplitude just before each application of ωCGVIA. The *bar* indicates the duration of toxin application. The *smooth lines* through the recovery data points are single-exponential fits. The recovery τ from each fit is listed beside the corresponding time course. *B*, Isochronic measurements of recovery from toxin block in 0, 3 μM, and 3 mM Ba^{2+}. Currents were measured at five points during recovery from ωCGVIA block (0, 30 sec, 1 min, 2 min, and 3 min) and normalized to that just before toxin application. Error bars indicate SD, and $n = 4$–10, except for recovery at 3 min for 0 Ba^{2+}, in which $n = 2$. $^{**}p < 0.01$ for all comparisons at that time.

charge carrier examined ($p < 0.01$). N-Current isolation in both Cs^+ and Na^+ was inferior to that in MA^+. This is clearly reflected in the smaller fraction of ωCGVIA-sensitive current in 0 Ba^{2+}–Na^+, but it was also true in 0 Ba^{2+}–Cs^+, in which it appeared that a noncalcium current generated a significant fraction of current at voltages depolarized to peak (data not shown). Our observations were not compromised by the poor isolation, because we are focusing on toxin blocking kinetics. However, other studies requiring isolated N-type current might be more difficult to interpret if either Cs^+ or Na^+ were used as the monovalent charge carrier.

The time course of block in 0 Ba^{2+}–Cs^+ was typically complete within 2 sec (Fig. 4*A*), which is the limit of our flow system. However, the blocking time course was significantly slower in 0 Ba^{2+}–Na^+ (3.7 ± 1.4 sec in Na^+ vs 1.9 ± 1.0 sec in MA^+) (Fig. 4*B*). Although N-current recovered from toxin block in both 0 Ba^{2+}–Cs^+ and 0 Ba^{2+}–Na^+, the time course was significantly slower than that in 0 Ba^{2+}–MA^+ ($p < 0.01$ for both Cs^+ and Na^+). Current in 0 Ba^{2+}–Cs^+ recovered from ωCGVIA block to 102 ± 8% of control with an average $\tau = 89 \pm 17$ sec ($n = 4$) (Fig. 4*A*). Surprisingly, the recovery time course in 0 Ba^{2+}–Na^+ was even slower, with a mean $\tau = 582 \pm 382$ sec ($n = 12$) (Fig. 4*B*). The current recovered to 89 ± 19% of control in 0 Ba^{2+}–Na^+, which was similar to that in 0 Ba^{2+}–MA^+. The estimation of the recovery τ in 0 Ba^{2+}–Na^+ was complicated by a persistent run up of N-current (ωCGVIA-sensitive current) in several cells. Although we are convinced that N-current recovers from ωCGVIA block in Na^+, we are not confident that we have an accurate measurement of the time course. However, it is clear from these data that the recovery of N-current from ωCGVIA block is not an artifact of using MA^+ as the monovalent charge carrier. The source of the differences in toxin blocking kinetics among these monovalent cations is unknown.

ωCGVIA off-rate is dependent on $[Ba^{2+}]_o$

To further test the notion that Ba^{2+} is the key factor in slowing recovery from ωCGVIA block, we examined the recovery from block at an intermediate $[Ba^{2+}]_o$. Addition of 3 μM Ba^{2+} to the external solution reduced the step current carried by MA^+ by ~40% at −20 mV (data not shown). Block of monovalent current by micromolar concentrations of divalent cations has been shown previously in N-channels (Carbone et al., 1997). The block can be explained with a model in which divalent cations interact at a high-affinity site along the permeation pathway to block monovalent current through calcium channels (Almers and McCleskey, 1984; Hess and Tsien, 1984; Dang and McCleskey, 1998). Application of ωCGVIA further blocked the current in 3 μM Ba^{2+}–MA^+ by 86 ± 2% ($n = 6$) (Fig. 5), similar to the block in 0 Ba^{2+}–MA^+ (88 ± 3%). The onset of ωCGVIA block in 3 μM Ba^{2+} could be fit with a single-exponential function (Fig. 5*A*). ωCGVIA blocked N-current in 3 μM Ba^{2+} with an average $\tau = 4 \pm 1$ sec ($n = 6$), which was significantly larger than that in 0 Ba^{2+} (2 ± 1 sec; $p < 0.05$). However, given that the exchange rate of our flow device is ~2 sec, the absolute difference in the blocking rate between 3 μM Ba^{2+} and 0 Ba^{2+} could not be

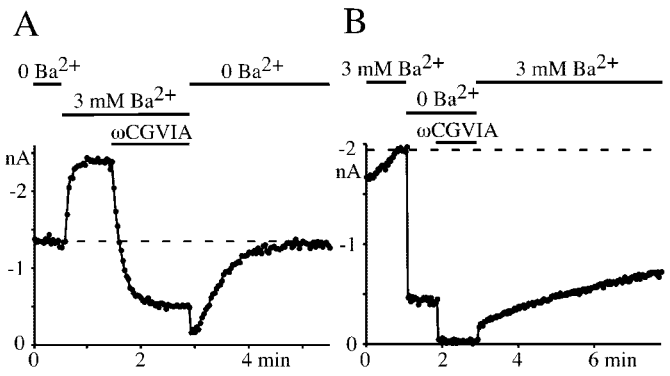

Figure 6. ωCGVIA does not occlude the Ba^{2+} binding site. *A*, Time course of ωCGVIA block in 3 mM Ba^{2+}–MA^+ and recovery from ωCGVIA block in 0 Ba^{2+}–MA^+. The *dashed line* indicates the current amplitude in the 0 Ba^{2+} control. *B*, Time course of toxin block in 0 Ba^{2+}–MA^+ and recovery from ωCGVIA block in 3 mM Ba^{2+}–MA^+. The *dashed line* indicates the current amplitude in the 3 mM Ba^{2+} control. In each *panel*, *solid bars* indicate change in $[Ba^{2+}]_o$ and/or application of 3 μM ωCGVIA.

reliably gauged for 3 μM ωCGVIA. We did not pursue the effect of $[Ba^{2+}]_o$ on the speed of block by ωCGVIA.

After removal of ωCGVIA, current returned to 75 ± 4% (n = 6) of that in 3 μM Ba^{2+} (Fig. 5*A*). The time course of recovery in 3 μM Ba^{2+}–MA^+ was well described by a single-exponential function with τ = 64 ± 16 sec (n = 6), which was significantly larger than that in 0 Ba^{2+}–MA^+ ($p < 0.05$). Isochronic measurement of relative current after ωCGVIA removal was used to compare the degree of recovery among 0 Ba^{2+}–MA^+, 3 μM Ba^{2+}–MA^+, and 3 mM Ba^{2+}–MA^+. The fractional current recovered was 0 Ba^{2+} > 3 μM Ba^{2+} > 3 mM Ba^{2+} (Fig. 5*B*). These results support the idea that micromolar $[Ba^{2+}]_o$ slows the dissociation of ωCGVIA from N-channels.

The Ba^{2+} binding site is not occluded by ωCGVIA

The finding that 3 μM Ba^{2+} slowed the recovery of N-current from ωCGVIA block suggests that the EC_{50} of Ba^{2+} would occur at micromolar $[Ba^{2+}]_o$, which is comparable to the block of MA^+ permeation by Ba^{2+} inside the pore. Apart from sites inside the pore, potential sites for Ba^{2+} binding also exist on the extracellular surface of the channel protein, such as those in which Ba^{2+} binds to screen surface charge (Zhou and Jones, 1995). We examined the location of the Ba^{2+} binding site that affects toxin block by changing the external solution at the time of toxin removal. In a simple model in which ωCGVIA is assumed to be a pore blocker, Ba^{2+} interaction sites inside the pore are isolated from the external solution once the toxin blocks the channel. These sites are exposed to Ba^{2+} only when Ba^{2+} enters the channels before toxin block. The hypothesis that Ba^{2+} interacts with sites inside the pore leads to the prediction that recovery from ωCGVIA block should be slow if 3 mM Ba^{2+} is used as the charge carrier during the block, regardless of the solution present during toxin washout. Alternatively, if the Ba^{2+} interaction site is located on a portion of the channel not occluded by ωCGVIA (such as the surface of the channel protein), it will be occupied only if Ba^{2+} is in the external solutions during wash off. The prediction from the second scenario is that unblock will be slow only if ωCGVIA is removed in the presence of 3 mM Ba^{2+}, regardless of the conditions during block.

In the first paradigm, the toxin was applied in 3 mM Ba^{2+}–MA^+ and washed off in 0 Ba^{2+}–MA^+ (Fig. 6*A*). After switching from 3 mM Ba^{2+}–ωCGVIA to 0 Ba^{2+}, there was an initial drop in the current amplitude caused by lower permeability of MA^+ through unblocked channels, but the ωCGVIA-blocked current recovered rapidly and completely. The recovery τ in 0 Ba^{2+} after block in 3 mM Ba^{2+} was 34 ± 8 sec, similar to the recovery τ in 0 Ba^{2+} after block in 0 Ba^{2+} (32 ± 3 sec) from the same three cells. The result suggests that Ba^{2+} binding at sites inside the channel pore does not slow the toxin dissociation. However, because 10 mM EGTA was used in the intracellular solution, the absence of a Ba^{2+} effect could arise from a Ba^{2+} binding site deep inside the channel, in which the local $[Ba^{2+}]$ is effectively controlled by the chelator. Alternatively, because ωCGVIA carries a +5 charge, toxin binding may have expelled Ba^{2+} from the interaction site in the channels. To test the model further, a second paradigm was used, in which ωCGVIA was applied in 0 Ba^{2+} and removed in 3 mM Ba^{2+}. The block in 0 Ba^{2+}–MA^+ was fast, as shown previously (Fig. 6*B*), but unblock in 3 mM Ba^{2+}–MA^+ progressed slowly except for the initial increase in current size, which was a result of switching from 0 Ba^{2+} to 3 mM Ba^{2+}. One concern was that the recovery time course in Figure 6*B* appeared to be faster than those in Figures 2*A* and 3*B*, which could indicate that recovery in 3 mM Ba^{2+} after block in 0 Ba^{2+} is faster than recovery after block in 3 mM Ba^{2+}. To determine whether this was true, we did an in-cell comparison of recovery time course in 3 mM Ba^{2+} after block in both 0 Ba^{2+} or 3 mM Ba^{2+}. We measured the percentage current recovered in 2 min (from the first to the third minute of toxin wash). This method was used because the first minute of recovery was often contaminated by an increase in current that resulted from the switch from 0 Ba^{2+} to 3 mM Ba^{2+}. In three cells, 7 ± 4% of control current recovered in 3 mM Ba^{2+} after block in 0 Ba^{2+}, which was statistically similar to the 4 ± 1% ($p > 0.05$) of current recovered in 3 mM Ba^{2+} after block in 3 mM Ba^{2+} in the same three cells. Thus, the presence of Ba^{2+} during ωCGVIA application did not appear to affect the toxin off-rate in either 0 Ba^{2+}–MA^+ or 3 mM Ba^{2+}–MA^+ wash solutions. The results demonstrate that the toxin cannot occlude the site to which Ba^{2+} binds to slow ωCGVIA dissociation from N-channels.

DISCUSSION

ωCGVIA block of N-current exhibited rapid kinetics in divalent cation-free solutions. The presence of 3 mM Ba^{2+} in the external solution slowed both toxin block and recovery from block. During unblock, ωCGVIA off-rate was correlated with $[Ba^{2+}]_o$ in the washout solution. Assuming that ωCGVIA is a pore blocker, Ba^{2+} most likely modifies toxin dissociation by interacting with a site(s) on the extracellular surface of the N-channel.

Ba^{2+} effect on the development of ωCGVIA block

We showed that the ωCGVIA on-rate was decreased when $[Ba^{2+}]_o$ was increased from 0 to 3 mM Ba^{2+}. Previous experiments by other groups demonstrated additional slowing of the ωCGVIA block as $[Ba^{2+}]_o$ was increased up to 110 mM (Boland et al., 1994; Elmslie et al., 1994). These studies in functional N-channels supported previous binding assays showing that increases in divalent cation concentration reduced the on-rate of radiolabeled toxin (Cruz and Olivera, 1986; Wagner et al., 1988; Witcher et al., 1993). Collectively, these results demonstrated that Ba^{2+} prolongs the time to equilibrium between ωCGVIA and N-channels. The effect of Ba^{2+} on toxin blocking rate does not appear to be sensitive to differences in experimental conditions between binding and functional assays (see below).

In addition to Ba^{2+} concentration, the blocking kinetics appeared to be sensitive to the monovalent cation in the external solution. In 3 mM Ba^{2+}, block was significantly slower in the presence of NMG^+ than when MA^+ was the dominant monovalent cation. In 0 Ba^{2+}, ωCGVIA block was slower in Na^+ than in either MA^+ or Cs^+. We cannot determine whether there is a difference in the blocking time course in MA^+ versus Cs^+, because the speed of block in both monovalent cations was at the limit of our flow device.

The origin of altered blocking kinetics by the different monovalent cations is not clear, but it is possible that the differences result from interaction of Na^+ and NMG^+ with the N-channel. Polo-Parada and Korn (1997) demonstrated that Na^+ could block Ca^{2+} and Ba^{2+} flux through N-channels in chick DRG cells. In addition, Zhou and Jones (1995) concluded that NMG^+ block of N-channels could underlie the reduced current observed with increasing NMG^+ concentration. Thus, it is possible that Na^+ and NMG^+ have higher affinity than MA^+ for a site(s) on the channel that interferes with toxin block. Such interactions could also explain the slower recovery from ωCGVIA block in Cs^+ and Na^+ compared with MA^+.

Dissociation of ωCGVIA from N-channels

Binding assays showed that K_{off} was not altered as divalent cation concentration was increased (Cruz and Olivera, 1986). Once the toxin–channel complex was formed, it was extremely stable, and no appreciable dissociation was detected for several hours in toxin-free solutions, even in the presence of high concentrations of divalent and trivalent cations. The apparent K_d at steady state was well below 10^{-11} M, which was attributed to an infinitesimal K_{off} (Cruz and Olivera, 1986). Therefore, binding assays support the idea that ωCGVIA is a potent, irreversible N-channel blocker.

However, measurable ωCGVIA off-rate has been observed in several previous functional studies. First, in frog and rat sympathetic neurons, increasing $[Ba^{2+}]_o$ accelerated the N-current recovery from block (Boland et al., 1994; Elmslie et al., 1994). Second, in frog neurons isolated using protease XXIII digestion instead of dispase, a sizable portion of whole-cell current recovered from ωCGVIA block in 5 mM Ba^{2+}, whereas the onset of block was not changed (Boland et al., 1994). The off-rate of toxin in these cells was comparable with that in 0 Ba^{2+} in our experiments. The protease effect suggests a potential role of an extracellular component of N-channels in regulating toxin off-rate. Third, in N-channels expressed in *Xenopus* oocytes, the recovery of ωCGVIA-blocked current could be accelerated by holding the membrane at hyperpolarized potentials (Stocker et al., 1997). This observation was explained by a model in which binding of ωCGVIA to N-channels is state dependent, and the apparent affinity of the toxin for inactivated channels is higher than for noninactivated channels (Stocker et al., 1997). Fourth, mutation of a single amino acid residue G1326P on the α_{1B} subunit produced channels that recovered rapidly from ωCGVIA block (Feng et al., 2001b). In contrast to binding assays, these functional experiments demonstrated that the reversibility of ωCGVIA depends on such factors as ionic conditions and N-channel conformation.

The apparent discrepancy in the reversibility of ωCGVIA between binding and functional assays could arise from their disparate experimental conditions. One difference is that neurons were homogenized before the membrane fraction was separated for measuring toxin binding. As a result, channel conformation–structure in membrane fractions may vary from that in intact neurons. More importantly, there is no negative resting potential resulting from the loss of membrane integrity and ionic gradients after homogenization. Thus, ωCGVIA binding was measured at 0 mV, which will inactivate the majority of N-channels. Recovery of current from inactivated N-channels has been shown to be significantly slower than from noninactivated channels (Stocker et al., 1997), which might explain the persistent binding of ωCGVIA to its receptor site in binding experiments. Conversely, functional studies were conducted on isolated neurons with well preserved cell membrane, and a negative holding potential was used to maintain stable N-current during experiments. Therefore, apparent discrepancy between binding and function studies may result from the dependence of ωCGVIA dissociation on channel conformation.

Ba^{2+} has biphasic effect on ωCGVIA dissociation

Previous findings from several groups together with the current observations demonstrated that ωCGVIA dissociation was sensitive to external divalent cations in a concentration-dependent manner (Boland et al., 1994; Elmslie et al., 1994). Intriguingly, these results suggest that the effect of external Ba^{2+} is biphasic. ωCGVIA dissociates rapidly in 0 Ba^{2+}, whereas the addition of moderate concentrations of Ba^{2+} (micromolar to low millimolar) slows unbinding. Increasing $[Ba^{2+}]_o$ from low millimolar to concentrations as high as 110 mM accelerates recovery from toxin block. In essence, ωCGVIA off-rate reached a nadir when external divalent cation concentration was within the physiological range. The effect of Ba^{2+} to decrease toxin off-rate probably involves the interaction site on the extracellular surface of N-channels, but the mechanism by which increased $[Ba^{2+}]_o$ accelerates off-rate remains to be determined (Boland et al., 1994).

Molecular basis of Ba^{2+} effects on ωCGVIA dissociation

It is unlikely that Ba^{2+} binds to ωCGVIA to slow toxin-association kinetics, because ωCGVIA carries five positive charges, which would electrostatically repulse Ba^{2+}. Moreover, there is no structural basis on the toxin for stabilizing Ba^{2+}, such as an EF-hand motif that can provide carboxyl oxygens to form coordinating sites for divalent cations.

Conversely, an EF-hand like Ca^{2+}-binding domain is present on the extracellular loop in domain III of the N-channel (α_{1B} subunit) (Feng et al., 2001a,b). This site overlaps the IIIS5–H5 region containing amino acid residues crucial for ωCGVIA binding (Ellinor et al., 1994; Feng et al., 2001b). The existence of a putative Ca^{2+}-binding motif close to the toxin-binding domain provides a potential structural basis for modification of ωCGVIA kinetics by divalent cations. However, toxin unbinding was also slowed by Cs^+ and Na^+ relative to MA^+, so it is currently premature to ascribe these monovalent and divalent cation effects to a particular site.

Physiological significance of the external site for divalent cations

In the absence of divalent cations, N-channels appear to undergo a conformational change that is reflected in the accelerated off-rate of ωCGVIA. Thus, for N-channels, divalent cations not only permeate but perhaps also maintain the functional conformation of the channel. The relevant binding site for divalent cations appears to reside on the extracellular surface of the channel. Although we did not estimate the EC_{50} of Ba^{2+} at this putative extracellular site, the effect of 3 μM Ba^{2+} on slowing toxin

dissociation suggests that Ba^{2+} is potent in reversing the conformational change. Thus, in physiological solutions containing millimolar concentrations of Ca^{2+} and Mg^{2+}, the extracellular divalent cation-binding site would probably be saturated, which would ensure normal channel function. However, this site provides a potential source for N-channel modulation. We demonstrated potential conformational changes in the absence of divalent cations. It will be interesting to determine whether these conformational changes affect other channel properties.

REFERENCES

Almers W, McCleskey EW (1984) Non-selective conductance in calcium channels of frog muscle: calcium selectivity in a single pore. J Physiol (Lond) 353:585–608.

Boland LM, Morrill JA, Bean BP (1994) ω-conotoxin block of N-type calcium channels in frog and rat sympathetic neurons. J Neurosci 14:5011–5027.

Carbone E, Lux HD, Carabelli V, Aicardi G, Zucker H (1997) Ca^{2+} and Na^{+} permeability of high-threshold Ca^{2+} channels and their voltage-dependent block by Mg^{2+} ions in chick sensory neurones. J Physiol (Lond) 504:1–15.

Cruz LJ, Olivera BM (1986) Calcium channel antagonists: omega-conotoxin defines a new high affinity site. J Biol Chem 261:6230–6233.

Dang TX, McCleskey EW (1998) Ion channel selectivity through stepwise changes in binding affinity. J Gen Physiol 111:185–193.

Ellinor PT, Zhang JF, Horne WA, Tsien RW (1994) Structural determinants of the blockade of N-type calcium channels by a peptide neurotoxin. Nature 372:272–275.

Elmslie KS (1992) Calcium current modulation in frog sympathetic neurones: multiple neurotransmitters and G proteins. J Physiol (Lond) 451:229–246.

Elmslie KS, Kammermeier PJ, Jones SW (1992) Calcium current modulation in frog sympathetic neurons: L-current is relatively insensitive to neurotransmitters. J Physiol (Lond) 456:107–123.

Elmslie KS, Kammermeier PJ, Jones SW (1994) Reevaluation of calcium channel types and their modulation in sympathetic neurons. Neuron 13:217–228.

Fabiato A, Fabiato F (1979) Calculator programs for computing the composition of the solutions containing multiple metals and ligands used for experiments in skinned muscle cells. J Physiol (Paris) 75:463–505.

Feng ZP, Hamid J, Doering C, Jarvis SE, Bosey GM, Bourinet E, Snutch TP, Zamponi GW (2001a) Amino acid residues outside of the pore region contribute to N-type calcium channel permeation. J Biol Chem 276:5726–5730.

Feng ZP, Hamid J, Doering C, Bosey GM, Snutch TP, Zamponi GW (2001b) Residue Gly1326 of the N-type calcium channel alpha 1B subunit controls reversibility of omega-conotoxin GVIA and MVIIA block. J Biol Chem 276:15728–15735.

Hess P, Tsien RW (1984) Mechanism of ion permeation through calcium channels. Nature 309:453–456.

Jones SW (1987) Sodium currents in dissociated bull-frog sympathetic neurons. J Physiol (Lond) 389:605–627.

Jones SW, Marks TN (1989a) Calcium currents in bullfrog sympathetic neurons. I. Activation kinetics and pharmacology. J Gen Physiol 94:151–167.

Jones SW, Marks TN (1989b) Calcium currents in bullfrog sympathetic neurons. II. Inactivation. J Gen Physiol 94:169–182.

Kim JI, Takahashi M, Ohtake A, Wakamiya A, Sato K (1995) Tyr13 is essential for the activity of omega-conotoxin MVIIA and GVIA, specific N-type calcium channel blockers. Biochem Biophys Res Commun 206:449–454.

Kuffler SW, Sejnowski TJ (1983) Peptidergic and muscarinic excitation amphibian sympathetic synapses. J Physiol (Lond) 341:257–278.

Lew MJ, Flinn JP, Pallaghy PK, Murphy R, Whorlow SL, Wright CE, Norton RS, Angus JA (1997) Structure-function relationships of omega-conotoxin GVIA: synthesis, structure, calcium channel binding, and functional assay of alanine-substituted analogues. J Biol Chem 272:12014–12023.

Liang H, Elmslie KS (2001) E_f-current contributes to whole-cell calcium current in low calcium in frog sympathetic neurons. J Neurophysiol 86:1156–1163.

Martell AE, Smith RM (1974) Critical stability constants, Vol 1, Amino acids. New York: Plenum.

Polo-Parada L, Korn SJ (1997) Block of N-type calcium channels in chick sensory neurons by external sodium. J Gen Physiol 109:693–702.

Stocker JW, Nadasdi L, Aldrich RW, Tsien RW (1997) Preferential interaction of ω-conotoxins with inactivated N-type Ca^{2+} channels. J Neurosci 17:3002–3013.

Wagner JA, Snowman AM, Biswas A, Olivera BM, Snyder SH (1988) ω-Conotoxin GVIA binding to a high-affinity receptor in brain: characterization, calcium sensitivity, and solubilization. J Neurosci 8:3354–3359.

Witcher DR, De Waard M, Campbell KP (1993) Characterization of the purified N-type Ca^{2+} channel and the cation sensitivity of omega-conotoxin GVIA binding. Neuropharmacology 32:1127–1139.

Zhou W, Jones SW (1995) Surface charge and calcium channel saturation in bullfrog sympathetic neurons. J Gen Physiol 105:441–462.